

Received October 22, 2018, accepted November 12, 2018, date of publication November 16, 2018, date of current version December 27, 2018.

Digital Object Identifier 10.1109/ACCESS.2018.2881766

Sparse Channel Estimation of Underwater TDS-OFDM System Using Look-Ahead Backtracking Orthogonal Matching Pursuit

NAVEED UR REHMAN JUNEJO¹, HAMADA ESMAIEL², (Member, IEEE),
MINGZHANG ZHOU¹, HAIXIN SUN¹, JIE QI¹, AND JUNFENG WANG³

¹Key Laboratory of Underwater Acoustic Communication and Marine Information Technology, Ministry of Education, School of Information Science and Engineering, Xiamen University, Xiamen, China

²Department of Electrical Engineering, Faculty of Engineering, Aswan University, Aswan, Egypt

³Department of Information and Communication Engineering, School of Electrical and Electronic Engineering, Tianjin University of Technology, Tianjin, China

Corresponding authors: Haixin Sun (hxsun@xmu.edu.cn) and Jie Qi (qjie@xmu.edu.cn)

This work was supported by the National Natural Science Foundation of China under Grant 61671394 and Grant 61471309.

ABSTRACT Time division synchronization orthogonal frequency division multiplexing (TDS-OFDM) has been attractive due to its fast synchronization and efficient spectral efficiency over conventional cyclic prefix orthogonal frequency division multiplexing (OFDM) and zero padding OFDM. However, inter-block interference (IBI) affects its performance because of delay over multipath channels. To evade IBI, dual pseudo-random noise (DPN) sequences have been introduced that causes to reduce spectral and energy efficiency. But, DPN is unprepared for underwater acoustic (UWA) communication because of battery-based nature and limited bandwidth. To overcome these issues, this paper exploits compressive sensing theory algorithm for obtaining the time-varying channel state information by utilizing sparse property of UWA channels. In this paper, the IBI free region is utilized to estimate accurate UWA channel impulse response and mitigate its interference. Look-ahead backtracking orthogonal matching pursuit-based sparse channel estimation technique is proposed for underwater TDS-OFDM in a real sparse time-varying multipath channel (channel taps are randomly distributed). Furthermore, Doppler-shift of UWA channel is estimated and compensated by PN sequence in time domain. The performance of the proposed technique is evaluated and demonstrated through numerical computation of bit error rate (BER) and mean square error (MSE) using Monte Carlo iterations. Simulation analysis confirms the superiority of the proposed scheme not only in terms of BER and MSE over the conventional ones but also achieve high energy and spectral efficiency.

INDEX TERMS Channel estimation, underwater acoustic, TDS-OFDM, LABOMP, energy efficiency, spectral efficiency.

I. INTRODUCTION

The performance of underwater acoustic (UWA) channels is a challenging for reliable high data rate communication due to oceanic environment characteristics. Mainly, four communication technologies are used for underwater communications (UWCs): underwater optical communication, underwater electromagnetic communication, underwater magnetic induction communication and underwater acoustic communication. Optical communication natural features, such as severe absorption, scattering, and line of sight (LOS) communication restrict its applications to be only used in a clear water [1]. Ocean conductivity creates the harsh attenuation in Electromagnetic and magnetic

induction waves. And to overcome such attenuation, ultra-low frequency bands should be used. The acoustic is the widest technology used in UWC over decades that achieves long distances of tens of kilometers and several tens of meters communication for a few kHz transmission and in the case of high transmission frequency, respectively. Though, the acoustic waves have a limited bandwidth, high Doppler shift, propagation delay, and ambient noise effects [1], [2]. In spite of these problems, acoustic communication is still the most usable UWC technology.

Several issues need to be examined thoroughly while designing the underwater acoustic communication (UWAC) systems. For example, attenuation causes assimilation of

acoustic waves in water which limits the transmission distance of waves and promotes multiple paths due to signal's reflection from top and bottom of the water. Transmitter and receiver motion results in the Doppler's effect and noise which masks the signal and slabs the related data [3]. Also, underwater environments dynamics may occur due to severe environmental conditions including seasonal changes, variations in geography with respect to seabed relief, water currents, temperature and salinity, tides behavior, generations of internal waves, relative motion between acoustic devices etc. These all complex properties make an underwater acoustic signal to fluctuate non-uniformly. For such issues selection of error correction and modulation techniques are critical and highly desirable. These issues can be resolved by multicarrier modulation that mitigates the bandwidth limitation and delay spread of wide channel results in unwanted inter-symbol interference (ISI) in case of a single carrier UWAC system. It can equalize channel at less complexity but significant Doppler's effect leads to severe inter-carrier interference (ICI) problems [4], [5]. Multicarrier technique is a substitute to overcome the longtime delay which makes higher the symbol interval but reduces the ISI in the UWAC channel. In such multicarrier communication, channel estimation techniques have a great attention [6]–[8].

Orthogonal frequency-division multiplexing (OFDM) multicarrier communication technique can roughly be categorized into three types: cyclic-prefix (CP), zero-padding (ZP) and time domain synchronization (TDS) OFDM [9]–[11]. CP is used in CP-OFDM as a guard interval to mitigate the inter-block interference (IBI) in multipath channels [9], [11], it converts the linear convolution to be circular one and can be used to estimate the channel response. CP replaced by zeros in ZP-OFDM to tackle the channel null problem and saving power consumed in guard interval [12], while its channel estimation is performed by exploiting frequency-domain pilots. Pseudo-random noise (PN) sequence has been adopted in the TDS-OFDM system as a guard interval and also as a training sequence for channel estimation and synchronization which is known to transmitter and receiver. The advantage of TDS-OFDM is improving the spectral and energy efficiency by reducing the transmission overhead of the pilot signal [13]. To facilitate the channel estimation and synchronization implementation, the PN sequences utilized in time-frequency training (TFT) OFDM [11], [14].

In long-tap delay channel such as UWA channel, a long guard interval is required between transmitted OFDM blocks to avoid ICI and a long pilots signal are needed to estimate such type of channel. As, the underwater communications are battery based and researchers have tried very hard to increase the life of battery as much as possible. Hence, the multicarrier modulation used in UWAC should be a low-power consumption. Since, the main objective of the TDS-OFDM is energy and spectral saving, hence it can be one of the most candidate for UWAC. But unfortunately, the TDS-OFDM is suffering from the high bit error rate (BER) due to IBI between data blocks and PN training

sequence and this problem considered as the TDS-OFDM's main problem. Two major approaches have been proposed to mitigate this problem [15]. The first approach is based on a classical iterative algorithm for interference cancellation [16] along with extension without changes in frame structure of TDS-OFDM scheme [17]. Though, those methods achieve slightly improvements in results especially in long delay UWA channel [15]. In another approach, the structure of TDS-OFDM frame has been modified to cancel out the interference [15]. As an example, in order to achieve the significant reduction in interference, the redundant pilots in frequency-domain are allocated in the unique word OFDM (UW-OFDM) for the generation of time-domain training sequence [18]. But the interference reduction of OFDM data blocks to training sequence can not be removed. Alternatively, a simple and an efficient scheme dual PN sequences are utilized in TDS-OFDM, where two PN sequences are used as guard interval after every data block to overcome interference from data block of OFDM to the second PN sequence [19]. Dual PN time division synchronization orthogonal frequency division multiplexing (DPN-TDS-OFDM) is proved to be a simplest scheme which offers good performance. Currently, it is under extensive investigation along with hardware implementation for the evaluation of standard of digital terrestrial multimedia broadcast (DTMB) [15], [19], [20], but unfortunately it is unapplicable for UWA communication due to duplicate of the guard interval which loss the energy and spectrum. Compressive sensing (CS) theory is used to recover the sparse signal through the small number of observation [21], which is an efficient and effective way to get better spectral efficiency [22]. The channel impulse response (CIR) is sparse in nature because the multipath delays are smaller than the channel delay spread [23]. This motivates to apply CS theory for sparse channel estimation [22], [24], [25].

In this paper, thanks to the sparsity nature of the UWA channel, CS method is proposed to estimate the channel from a small IBI free region in the TDS-OFDM training sequence. Firstly, the Doppler factor is estimated then compensated by the received PN sequence in time domain. Secondly, the channel is estimated using sparse recovery greedy algorithm look-ahead backtracking orthogonal matching pursuit (LABOMP) with an IBI free region in the real sparse time-varying multipath UWA channel. IBI free region is used as an interference mitigation region to reconstruct the real sparse channel effectively and efficiently. The purpose of choosing LABOMP is showing a better signal recovery from the small IBI free region. Simulation results validate our analysis and exhibit that, the proposed technique attains higher spectral and energy efficiency, less BER, MSE, and also getting higher data rate in comparison to conventional TDS-OFDM and DPN-TDS-OFDM systems.

The rest of the paper is organized as follows: the details of system model of TDS-OFDM including UWA channel model, time synchronization, coarse Doppler scaling factor, Doppler shift estimation, and the considered LABOMP

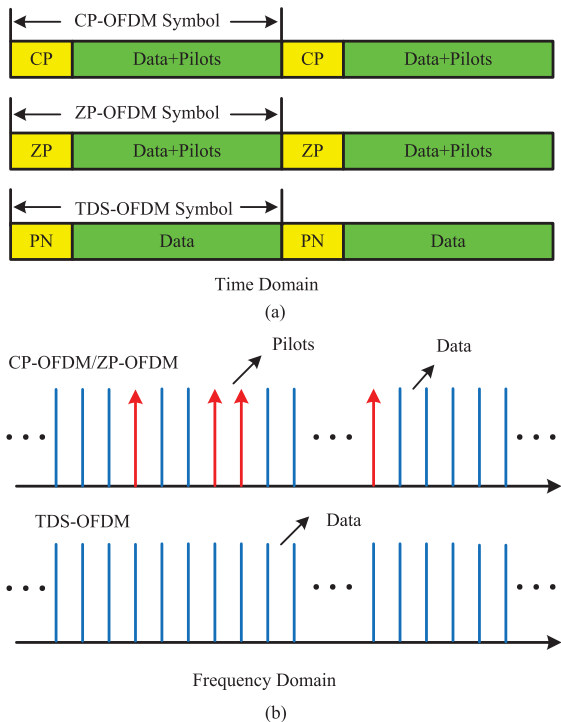


FIGURE 1. CP-OFDM, ZP-OFDM and TDS-OFDM signal structure (a) time-domain (b) frequency-domain.

based channel estimation are described in section II and III respectively. Experimental results and discussion is described in section IV. Finally, the conclusion is drawn in section V.

II. SYSTEM MODEL

The comparison of TDS-OFDM, CP-OFDM, and ZP-OFDM signals structure in frequency and time domain are shown in Fig. 1, where TDS-OFDM, CP-OFDM and ZP-OFDM used PN sequence, CP and ZP as a guard interval respectively. Symbol of TDS-OFDM contains OFDM data and PN sequence whereas the PN sequence is a cyclic prefix for the data of OFDM. The length of the guard band needs to be longer as compared to the maximum excess delay of multiple path channels so that data does not influence from IBI. IBI free region is being used before the data block of OFDM that corresponds performance loss. The PN sequence for the i^{th} block can be represented as:

$$\mathbf{c}_i = \{c_{i,k}\}_{k=0}^{M-1}, \tag{1}$$

where M is the length of PN sequence, the i^{th} OFDM data block can be defined as:

$$\mathbf{x}_i = \{x_{i,k}\}_{k=0}^{N-1}, \tag{2}$$

where k is the k^{th} element of the i^{th} TDS-OFDM data block, N is the length of OFDM data block, and such transmitted frame can be defined as:

$$\mathbf{s}_i = [s_{i,0}, s_{i,1}, \dots, s_{i,M+N-1}]^T = [\mathbf{c}_i, \mathbf{x}_i]_{M+N \times 1}^T, \tag{3}$$

A. CHANNEL MODEL

The UWA channel is considered as time-varying multipath channel and its impulse response can be defined as [26]–[28]:

$$h_i(t, \tau) = \sum_k A_{i,k}(t)\delta(\tau - \tau_{i,k}(t)), \tag{4}$$

where $\tau_{i,k}(t)$ and $A_{i,k}(t)$ are the time-varying path delay and path amplitude, respectively. This channel model consists of multiple important paths; every path is parameterized by time-varying path delay and path amplitude. Assume the following conditions for the simplicity of the receiver process algorithms development without loss of generality.

1) All paths delays $\tau_{i,k}(t)$ have a similar Doppler scaling factor (DSF) as:

$$\tau_{i,k}(t) = \tau_{i,k} - \beta_i t, \tag{5}$$

where β_i is DSF. Generally, total different paths may have different DSF. In this paper, the method which we have considered for DSF is based on the assumption that each of the path has the similar DSF.

2) The path amplitudes $A_{i,k}(t)$ remain constant within the same block duration as:

$$A_{i,k}(t) = A_{i,k}. \tag{6}$$

In this paper, the channel parameters, path amplitude $A_{i,k}(t)$, path delay $\tau_{i,k}(t)$ and DSF β are assumed to vary slowly throughout the whole transmission.

B. TIME SYNCHRONIZATION AND COARSE DOPPLER SCALING FACTOR ESTIMATION

A joint time synchronization and coarse DSF estimation method exploits the embedded repetitive pattern in transmitted preamble \mathbf{c}_i that reported in [27] and [28] is adopted in our system. The corresponding correlation P-tap window can be formulated as:

$$(\hat{p}_i, \hat{d}_i) = \arg \max_{P,d} \frac{\sum_{p=d}^{d+P-1} \mathbf{r}_{i,p}^* \mathbf{r}_{i,p+P}}{\sqrt{\sum_{p=d}^{d+P-1} |\mathbf{r}_{i,p}|^2 \sum_{p=d}^{d+P-1} |\mathbf{r}_{i,p+P}|^2}}, \tag{7}$$

where $r_{i,p}$ is the baseband equivalence of the received passband signal sampled at a rate αB with an integer parameter α and \hat{d}_i is the beginning time of the received preamble signal. The integer \hat{P}_i yields a coarse estimate of initial tap delay $\beta_{i,0}$ as discussed in [27]:

$$\bar{\beta}_{i,0} = \frac{\alpha N - \hat{P}_i}{\hat{P}_i}, \tag{8}$$

The estimator (8) can only offer time synchronization and DSF estimation with a precision limit α . In OFDM system after the passband-to-baseband conversion, a small timing error amounts in the phase offset occur. In this paper, through the use of time domain PN sequence this phase offset is estimated and compensated. Meanwhile, the small DSF error estimation can lead to a significant IBI and ICI.

C. DOPPLER SHIFT ESTIMATION

The effects of the DSF can be largely mitigated by re-sampling the received preamble data in passband at a re-sampling rate $(\bar{\beta}_{i,0} + 1)B$ [27]. The resulting converted baseband signal is given by:

$$\mathbf{z}_{i,n} = e^{j2\pi \frac{\beta_{i,0} - \bar{\beta}_{i,0}}{1 + \bar{\beta}_{i,0}} \times \frac{F_c}{B}} \sum_n \mathbf{h}_{i,n} \mathbf{c}_{i,n} e^{j\frac{2\pi n p}{N}}, \quad (9)$$

where F_c is the carrier frequency, B is the bandwidth and $\mathbf{h}_{i,n}$ is the sub-channel gain at the n -th subcarrier and can be denoted as:

$$\mathbf{h}_{i,n} = \sum_k A_{i,k} e^{-j2\pi(F_c + n\Delta F)\tau_{i,k}}. \quad (10)$$

The Doppler shift can be represented as:

$$\epsilon_{i,0} = \frac{\beta_{i,0} - \bar{\beta}_{i,0}}{1 + \bar{\beta}_{i,0}} \times \frac{F_c}{B}, \quad (11)$$

it is assumed that $1 + \beta_{i,0}/1 + \bar{\beta}_{i,0} \approx 1$ to account for possible errors in coarse DSF estimation and the approximation. As $\mathbf{z}_{i,p+N} = \mathbf{z}_{i,p} \exp(j2\pi\epsilon_{i,0}N)$ for $0 < p \leq N - 1$, an estimator of $\epsilon_{i,0}$ can be formulated as:

$$\hat{\epsilon}_{i,0} = \frac{\sum_{p=0}^{N-1} \angle(\mathbf{z}_{i,p+N} \mathbf{z}_{i,p}^*)}{2\pi N^2}. \quad (12)$$

In [29], the Doppler shift estimation is conducted by using additional null subcarriers but our considered Doppler shift estimation solely depends on the special structure already embedded within the preamble. Given estimates $\bar{\beta}_{i,0}$ and $\epsilon_{i,0}$; an estimate of the overall DSF $\beta_{i,0}$ can be obtained as:

$$\hat{\beta}_{i,0} = \bar{\beta}_{i,0} + \frac{B}{F_c} (1 + \bar{\beta}_{i,0}) \hat{\epsilon}_{i,0}. \quad (13)$$

III. COMPRESSIVE SENSING TECHNIQUE FOR TDS-OFDM UWA CHANNEL

A. MOTIVATION

In the TDS-OFDM scheme, the interference contains different features such that if the data block of OFDM is unknown so it is difficult to get perfect detection over multipath channels as depicted in Fig. 2. It is highly challenging to mitigate IBI completely occur due to the data block of OFDM even with perfectly employed channel estimation techniques. Moreover, OFDM data block possesses large size due to which calculating IBI require high computational complexity. On the contrary, since the receiver knows training sequence, the IBI exploited by the training sequence can be incisively computed only when channel estimation has been attained accurately. This statement provokes the issue of intractable mutual interference for estimating channel accurately solved by ignoring the effect of OFDM data block to training sequence. In practical applications, we also discover that the small IBI free region exists within the received training sequence due to the system margin design. The worst case scenario in TDS-OFDM and CP-OFDM occurs when the

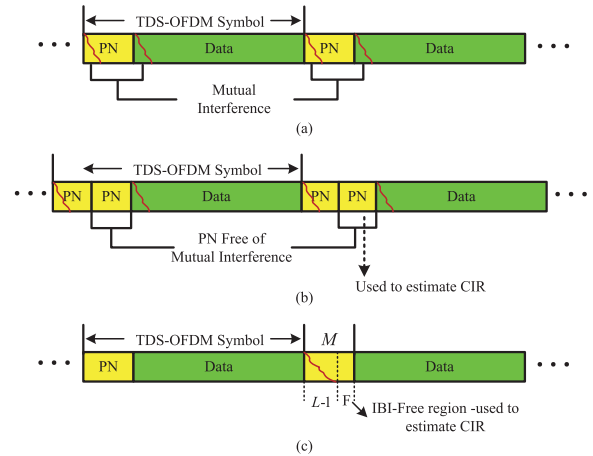


FIGURE 2. Received signal frame structure (a) Conventional TDS-OFDM (b) DPN-TDS-OFDM (c) CS based TDS-OFDM.

guard interval has the equivalent channel length. In order to combat the worst case, to evade the IBI and also for perfect estimation, the channel length should be smaller than the guard interval. Our proposed transceiver model is shown in Fig. 3.

With perfect channel estimation, the mutual interference can be eliminated entirely from the data block of the TDS-OFDM. As such, both the TDS-OFDM and ZP-OFDM will be equivalent after subtraction of PN sequence. The affect of mutual interference from data block to PN sequence in the conventional TDS-OFDM is solved by using the DPN-TDS-OFDM technique. In a DPN-TDS-OFDM frame the guard interval is duplicated to receive a PN sequence without IBI, and based on such free PN sequence a perfect channel estimation can be obtained. Fig. 2 shows the difference between the received frames of these TDS-OFDM schemes over multipath channels. As shown in Fig. 2, (a), the received PN sequence is affected by IBI because of former data block OFDM in multipath channels and this interfered PN sequence is used in channel estimation. Channel estimation in time domain is performed for the TDS-OFDM and the received PN sequence can be written as:

$$\mathbf{r}_i = \Psi_i \mathbf{h}_i + \mathbf{v}_i, \quad (14)$$

here \mathbf{v}_i is additive white Gaussian noise (AWGN) and Ψ_i should be written as:

$$\Psi_i = \begin{bmatrix} c_{i,0} & x_{i-1,N-1} & \dots & x_{i-1,N-L+1} \\ c_{i,1} & c_{i,0} & \dots & x_{i-1,N-L+2} \\ \vdots & \vdots & \ddots & \vdots \\ c_{i,L-1} & c_{i,L-2} & \dots & c_{i,0} \\ c_{i,L} & c_{i,L-1} & \dots & c_{i,1} \\ \vdots & \vdots & \ddots & \vdots \\ c_{i,M-1} & c_{i,M-2} & \dots & c_{i,M-L} \end{bmatrix}_{M \times L} \quad (15)$$

The propagation paths K are the sparsity of channel, which are required to be small for exact recovery using

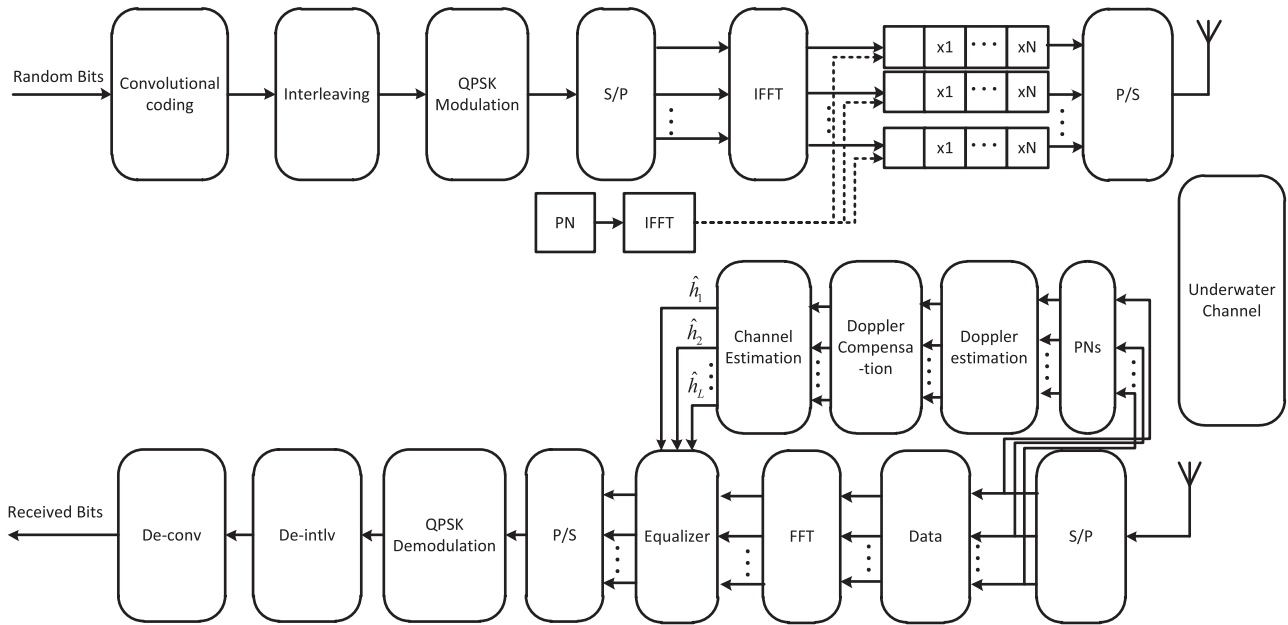


FIGURE 3. Block diagram of proposed underwater TDS-OFDM transceiver.

CS theory [30], [31]. However, channel sparsity is to be decided by the length of channel L and observations F (number of rows), not only by number of channel taps K . The sparsity of channel must satisfy the condition of restricted isometry principle less (RIPless) for the secure channel estimation and can be computed as:

$$K \leq \frac{F}{4C_0(\log(L/F) + 1)}, \quad (16)$$

here C_0 is the universal constant which is approximate to 1 and it can be adjusted according to the various situation and CS matrix.

Noting that in (15), $(i-1)^{th}$ components represent to previous transmitted block which interferes the current TDS-OFDM symbol. Meanwhile, it can also notice that the previous data block of TDS-OFDM does not contaminate the last samples $M - L + 1$ of received PN sequence. Therefore, CS theory estimates the channel by using the IBI free region. Here, we extort the last $F = M - L + 1$ rows of Ψ_i to make new sub-matrix named as the observation-matrix, it can be written as:

$$\Phi_i = \begin{bmatrix} c_{i,L-1} & c_{i,L-2} & c_{i,L-3} & \dots & c_{i,0} \\ c_{i,L} & c_{i,L-1} & c_{i,L-2} & \dots & c_{i,1} \\ \vdots & \vdots & \vdots & \ddots & \vdots \\ c_{i,M-1} & c_{i,M-2} & c_{i,M-3} & \dots & c_{i,M-L} \end{bmatrix}_{F \times L}, \quad (17)$$

here the observation matrix $F \times L$ size determined by the PN sequence. Finally, the received signal is corrupted by noise in IBI free region and can be denoted as:

$$\mathbf{y}_i = \Phi_i \mathbf{h}_i + \mathbf{v}_i. \quad (18)$$

Algorithm 1 Look-Ahead Residue

Input: $\Phi \in \mathbb{R}^{F \times L}$, $\mathbf{y} \in \mathbb{R}^{F \times 1}$, Sparsity K , previous support set \mathbf{I} , newly selected index i ;

Initialization: the intermediate support set $\mathbf{I}_k = \mathbf{I}_k \cup i$, the approximate coefficient $\hat{\mathbf{h}}_{I_k} = \Phi_{I_k}^\dagger \mathbf{y}$, residual $\mathbf{r}_k = \mathbf{y} - \Phi_{I_k} \cdot \hat{\mathbf{h}}_{I_k}$, counter $k = |\mathbf{I}_k|$;

Repeat:

- 1: $k = k + 1$;
- 2: $i_k = \arg \max_{i=1}^N \Phi_i^T \mathbf{r}_{k-1}$, $i \notin \mathbf{I}_{k-1}$; % matched filter
- 3: $\mathbf{I}_k = \mathbf{I}_k \cup i$; % update the support set
- 4: $\hat{\mathbf{h}}_{I_k} = \Phi_{I_k}^\dagger \mathbf{y}$; % estimate signal \hat{h}_{I_k}
- 5: $\mathbf{r}_k = \mathbf{y} - \Phi_{I_k} \hat{\mathbf{h}}_{I_k}$; % estimate residue r_k

Until $\|\mathbf{r}_k\|_2 > \|\mathbf{r}_{k-1}\|_2$ or $k > K$

Output: $\mathbf{r}_k = \mathbf{y} - \Phi_{I_k} \Phi_{I_k}^\dagger \mathbf{y}$;

B. LOOK-AHEAD BACKTRACKING ORTHOGONAL MATCHING PURSUIT

As the free IBI region in TDS-OFDM should be small as much as we can to save energy and spectrum in UWA communication. This paper proposes the LABOMP algorithm for channel estimation by using the small IBI free region. According to LABOMP algorithm [32], the look-ahead residue scheme and the backtracking scheme are implemented by utilizing the look ahead residue (LAR) function and the backtrack pruning (BP) function respectively. The procedure of LAR function in algorithm 1. Firstly, a fixed look-ahead parameter LL is set to choose the potential LL atoms which are most correlative with the residue of the last iteration. Secondly, the effect of each potential atom is predicted respectively for the final fitting residue, and the best

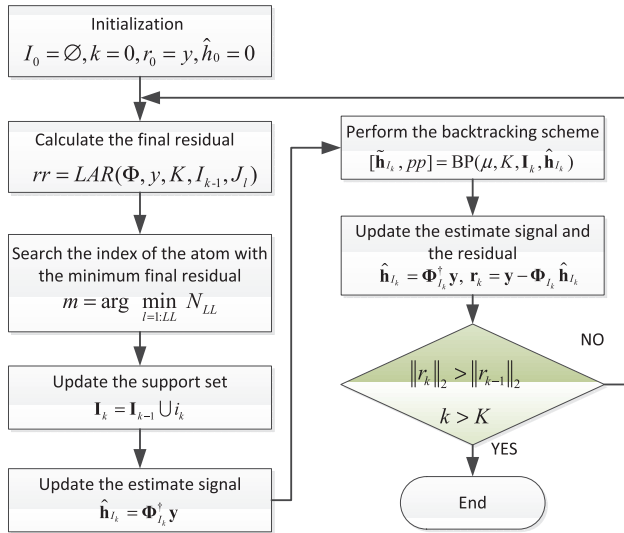


FIGURE 4. LABOMP algorithm.

Algorithm 2 The Backtracking Pruning

Input: $\mu, K, \mathbf{I}_k, \hat{\mathbf{h}}_{I_k}$;
Initialization: $\lambda = \mu K$;
if $k \geq \lambda$ & $k \% 2 = 1$
 1: $[v, pp] = \arg \min |\hat{\mathbf{h}}_{I_k}|$;
 2: $\mathbf{I}_k = \mathbf{I}_k \setminus pp$; % eliminate the minimum $\hat{\mathbf{h}}_{I_k}$
end if
Output: \mathbf{I}_k, pp

one is put into the support set. Thirdly, the estimated signal and the residue are updated. Finally, the algorithm determines whether the current iteration satisfies the terminated condition [33]. LABOMP algorithm given in Fig. 4.

The algorithm 1, can be used by defining the following functions. Function 1 (Look ahead residual) set $\mathbf{y} \in \mathbb{R}^{F \times 1}$, $\Phi \in \mathbb{R}^{F \times L}$ and K is the sparsity level. The set of the intermediate support defined formerly is \mathbf{I} , and optimal atom index in the present iteration is i . Then we can use the following algorithmic function to obtain the output residual $\mathbf{rr} \in \mathbb{R}^F$,

$$\mathbf{rr} = LAR(\mathbf{y}, \mathbf{A}, K, \mathbf{I}, \mathbf{J}_l). \tag{19}$$

Function 2 (the backtracking pruning). Let $\mu \in [0, 1]$ and the sparsity level K . Consider that the current chosen set of the intermediate support is \mathbf{I}_k and the estimated signal passing the LAR function is $\hat{\mathbf{h}}_{I_k}$. Then we can use the following algorithmic function to obtain the new index of atoms \mathbf{I}_k and the backtracking index k .

$$[\mathbf{I}_k, pp] = BP(\mu, K, \mathbf{I}_k, \hat{\mathbf{h}}_{I_k}). \tag{20}$$

By backtracking scheme, all iterations can be classified into two types, which includes a dominant look-ahead convergence and cascade backtracking. Assume that $\lambda = \mu \cdot K$, where λ is a preset constant threshold that triggers the stage of cascade backtracking to delete wrong atoms selected in previous iterations. λ is correlated with the signal structure

Algorithm 3 Look-Ahead Backtracking Orthogonal Matching Pursuit

Input: $\Phi, \mathbf{y}, K, \lambda, ;$
Initialization: $I_0 = \emptyset, k = 0, LL = 5, r_0 = y, \hat{h}_0 = 0$;
Repeat:
 1: $k = k + 1$;
 2: $\mathbf{A}_n = \Phi_i^T \mathbf{r}_{k-1}$ % match filter
 3: $\mathbf{J} = \text{supp}((\mathbf{A}_n)_{LL})$;
 for $l = 1 : LL$
 4: $\mathbf{rr} = LAR(\mathbf{y}, \mathbf{A}, K, \mathbf{I}, \mathbf{J}_l)$;
 5: $\mathbf{N}_l = \|\mathbf{rr}\|_2$;
 end for
 6: $m = \arg \min_{l=1}^{LL} \mathbf{N}_{LL}$; % update the support set
 7: $i_k = \mathbf{J}_m$;
 8: $\mathbf{I}_k = \mathbf{I}_{k-1} \cup i_k$;
 9: $\hat{\mathbf{h}}_{I_k} = \Phi_{I_k}^\dagger \mathbf{y}$; % estimate signal
 if $k \geq \lambda$ & $k \% 2 = 1$; % search space of backtracking strategy
 10: $[\mathbf{I}_k, pp] = BP(\mu, K, \mathbf{I}_k, \hat{\mathbf{h}}_{I_k})$;
 end if
 11: $\hat{\mathbf{h}}_{I_k} = \Phi_{I_k}^\dagger \mathbf{y}$;
 12: $\hat{\mathbf{h}}_{I_k} = \Phi_{I_k}^\dagger \mathbf{y}$;
 13: $k = pp - 1$;
Until $\|\mathbf{r}_k\|_2 > \|\mathbf{r}_{k-1}\|_2$ or $k > K$
Output: $\mathbf{h}_{I_k}, \mathbf{r}_k$

and the rule of adding the atom. Therefore, $\lambda = 0.8K \sim 0.9K$ is reasonable empirical value for LABOMP algorithm. The main idea of BP function is elaborated in algorithm 2. Firstly, correct large coefficient atoms can be captured in the stage of dominant look-ahead convergence. Secondly, because the mismatched atoms with the small coefficients are not strict orthogonal, which are selected in previous iterations, the backtracking scheme is performed to prune most mismatching atoms from the support set [32]. Considering the T consecutive TDS-OFDM symbols with IBI free region having same sequence of PN i.e. $\mathbf{c}_i = \mathbf{c}_{i+1} = \dots \mathbf{c}$ which leads to $\Phi_i = \Phi_{i+1} = \dots = \Phi$, the (18) can be written as:

$$\mathbf{Y} = \Phi \mathbf{H} + \mathbf{V}, \tag{21}$$

where

$$\mathbf{Y} = [\mathbf{y}_i, \mathbf{y}_{i+1}, \dots, \mathbf{y}_{i+T-1}]_{F \times T},$$

$$\mathbf{V} = [\mathbf{v}_i, \mathbf{v}_{i+1}, \dots, \mathbf{v}_{i+T-1}]_{F \times T},$$

Recently, the standard CS theory [34] has been extended with new concept known as structured CS shown in (22). Therefore, the multiple channels in \mathbf{H} , that are grouped together exploit joint sparsity can be recovered by using simultaneous optimization problem [35] as:

$$\tilde{\mathbf{H}} = \arg \min_{\mathbf{H} \in \mathbb{C}^{L \times T}} \|\mathbf{H}\|_{p,q}, \tag{22}$$

where matrix $\hat{\mathbf{H}}$ quasi-norm can be calculated as:

$$\|\mathbf{H}\|_{p,q} = \left(\sum_i \|\mathbf{m}_i\|_p^q \right)^{1/q}, \quad (23)$$

where \mathbf{m}_i is the i^{th} row of the \mathbf{H} . Generally, CS norm is used means $p = 0$ and $q = 1, 2$. When $T = 1$ the (21) reduces to be (18) but for the reliable recovery of the signal the required observations number will be increased from $O(K)$ to $O(K \log_2(L/K))$ for $T > \log_2(L/K)$ [36].

C. ESTIMATION BASED ON MAXIMUM LIKELIHOOD

In the maximum-likelihood estimation-based, the path delay is estimated then the received signal model of (18) is written as:

$$\mathbf{y}_i = \Phi_i(\mathbf{h}_i + (\Phi_i^H \Phi_i)^{-1} \Phi_i^H \mathbf{v}_i), \quad (24)$$

$$\mathbf{h}_i = (\Phi_i^H \Phi_i)^{-1} \Phi_i^H \mathbf{y}_i - (\Phi_i^H \Phi_i)^{-1} \Phi_i^H \mathbf{v}_i = \Phi_i^\dagger \mathbf{y}_i - \Phi_i^\dagger \mathbf{v}_i, \quad (25)$$

where $\Phi_i^\dagger = (\Phi_i^H \Phi_i)^{-1} \Phi_i^H$ expresses the pseudo-inverse of Φ_i . In general, linear estimation of channel techniques are directly designed to approach $\mathbf{h}_i + (\Phi_i^H \Phi_i)^{-1} \Phi_i^H \mathbf{v}_i$, thus the performance is restricted by the contamination of the equivalent noise $(\Phi_i^H \Phi_i)^{-1} \Phi_i^H \mathbf{v}_i$ in (24). The advantage of nonlinear estimation methods based on CS is the ability of reconstruction of sparse channel and avoidance interference part caused by the equivalent noise $(\Phi_i^H \Phi_i)^{-1} \Phi_i^H \mathbf{v}_i$. CS algorithm conceptualizes with the iterative exploration of the strongest channel taps to the weakest one [37]. As such when the channel taps are weak, it is not easy to decide whether the explored taps are true. According to (25), we have $\Phi_i^\dagger \mathbf{v}_i$ that can easily be achieved as $E\{\Phi_i^\dagger \mathbf{v}_i\} = E\{\Phi_i^\dagger\} E\{\mathbf{v}_i\} = 0$, the measurement matrix Φ_i , and the noise vector \mathbf{v}_i are independent. After that, in equivalent noise $\Phi_i^\dagger \mathbf{v}_i$ the covariance of the elements can be derived as:

$$Var\{\Phi_{ij}^\dagger \mathbf{v}_i\} = F Var\{\Phi_{ij}^\dagger\} Var\{\mathbf{v}_i\} = F \sigma_{\mathbf{v}_i}^2 Var\{\Phi_{ij}^\dagger\}, \quad (26)$$

where Φ_{ij}^\dagger is the j^{th} row of Φ_i^\dagger and Φ_{ij}^\dagger is the j^{th} element of Φ_i^\dagger . Furthermore, we have

$$\Phi_i^\dagger \mathbf{v}_i \sim CN(0, \sigma_{\Phi_i^\dagger \mathbf{v}_i}^2) \approx CN\left(\frac{F \sigma_{\mathbf{v}_i}^2}{L^2 \sigma_{\Phi}^2}\right). \quad (27)$$

IV. EXPERIMENTAL RESULTS AND DISCUSSION

We have investigated the effectiveness of TDS-OFDM free IBI region CS based LABOMP technique over other conventional techniques i.e. TDS-OFDM, DPN-TDS-OFDM, OMP and CoSaMP using the numerical computations of MSE and BER. For experiment FFT size is 1024, the signal bandwidth is 6KHz, and the PN sequence length is 255. Further parameters are mentioned in Table 1.

Fig. 5 shows the CIR estimation of LABOMP over real sparse time-varying channel comparing with OMP, CoSaMP

TABLE 1. System specifications.

Parameters	values
FFT size (N)	1024
Guard Interval PN sequence (M)	255
Channel Length (L)	180
IBI free region (F)	75
Bandwidth (B)	6KHz
Central Frequency (F_{cr})	30KHz
Sampling Frequency (F_s)	96KHz
Carrier Frequency (F_c)	20KHz
Carrier Frequency Offset (CFO)	0.2
Symbol Duration	170.67 msec
Data Rate	11.99 kbit/sec
Modulation	QPSK

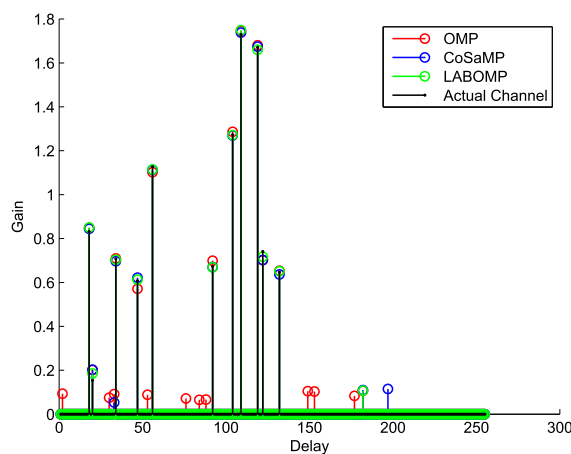


FIGURE 5. Estimated CIR of different CS methods over real sparse channel.

at 20 dB SNR. LABOMP estimation outperforms the OMP and CoSaMP in terms of path delay and path gain as shown in Fig. 5. Also, LABOMP has nearly exact CIR estimation, where it does not estimate channel taps when actual channel taps are not present. But, OMP and CoSaMP have many estimated channel taps with small gain when actual channel taps don't exist.

The MSE performance of LABOMP compared with conventional TDS-OFDM, DPN-TDS-OFDM, OMP and CoSaMP is shown in Fig. 6, at sparsity equals to 10, which meets the RIPless condition in (16). The MSE is calculated as:

$$MSE = \frac{E\{\sum_k |\hat{\mathbf{h}}_k - \mathbf{h}_k|^2\}}{E\{\sum_k |\hat{\mathbf{h}}_k|^2\}}. \quad (28)$$

In the conventional TDS-OFDM, the third iteration is carried out to cancel the iterative interference for the reliable channel estimation [16]. In the DPN-TDS-OFDM, the second PN sequence is used to estimate the channel [19]. For LABOMP, OMP and CoSaMP IBI free region is used to reconstruct the channel. As shown in Fig. 6, the LABOMP outperforms the basic TDS-OFDM and DPN-TDS-OFDM by about 5.89 dB and 4.29 dB, respectively, when target MSE is considered

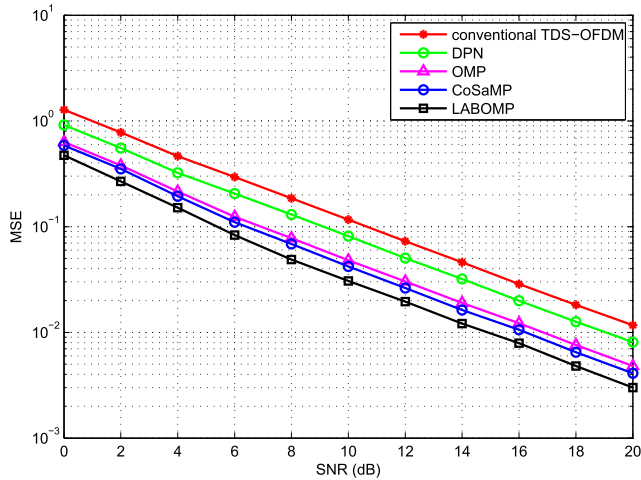


FIGURE 6. Channel estimation performance comparison of LABOMP with conventional TDS-OFDM, DPN-TDS-OFDM, OMP and CoSaMP for real sparse UWA channel with CFO K [1, 10].

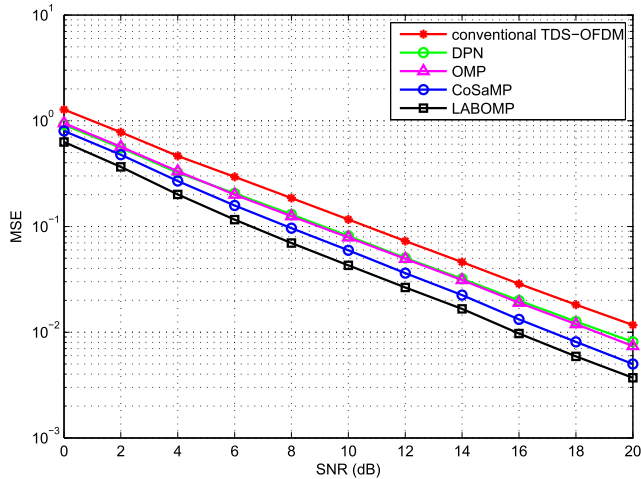


FIGURE 7. Channel estimation performance comparison of LABOMP with conventional TDS-OFDM, DPN-TDS-OFDM, OMP and CoSaMP for complex channel in case of CFO K [1, 20].

as 10^{-2} . Thanks to LABOMP capability to explore entire channel sparsity characteristics and estimate all UWA channel taps even in the presence of dominated noise, LABOMP outperforms the OMP and CoSaMP with a margin of 2.14 dB and 1.54 dB respectively.

In Fig. 7, the MSE performance of LABOMP, OMP, CoSaMP, DPN-TDS-OFDM and conventional TDS-OFDM has been compared over the extremely UWA complex channel, where channel sparsity is distributed uniformly as K [1, 20], the RIPless condition cannot meet $F/4C_0(\log(L/F) + 1)$. Here, sparsity slightly effects on the performance of the TDS-OFDM and DPN-TDS-OFDM, at MSE equal to 10^{-2} , the gain difference still same as in Fig. 6. The performance of CS based algorithms severely degraded compared to the conventional TDS-OFDM and DPN-TDS-OFDM schemes. However, the LABOMP

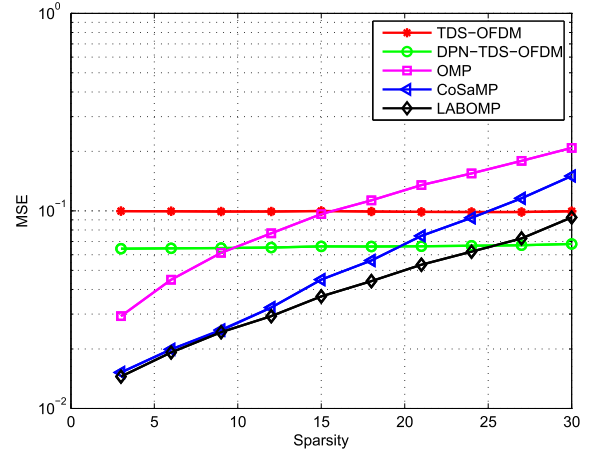


FIGURE 8. Channel estimation performance for different channel sparsity K .

outperforms the DPN-TDS-OFDM and conventional TDS-OFDM by about 3 dB and 4.6 dB SNR gain when MSE is considered 10^{-2} , respectively. In addition, LABOMP performance surpasses the CoSaMP and OMP by about 1.1 dB and 2.8 dB SNR gain when 10^{-2} MSE is targeted, respectively.

Fig. 8 shows the MSE performance for different channel sparsity at $SNR = 10$ dB, $PN = 255$, $F = 75$, and $L = 180$. The channel sparsity did not effect on the channel estimation performance of conventional TDS-OFDM and DPN-TDS-OFDM, so it is proved that these are not compressive sensing methods because MSE remains stable with various sparsity level. Although, the performance of CS methods like OMP, CoSaMP and LABOMP affected by the channel sparsity, it means that the performance is directly concerned with sparsity of channel. The CS methods perform better than conventional TDS-OFDM and DPN-TDS-OFDM when channel sparsity is $K \leq 14$ as (16). As shown in Fig. 8, a different sparsity thresholds for CS methods should be considered. LABOMP CS method performs better than conventional TDS-OFDM and DPN-TDS-OFDM up to channel sparsity $K = 25$. But in case of OMP and CoSaMP this sparsity threshold is up to $K = 10$ and $K = 20$ respectively, to outperform the conventional TDS-OFDM and DPN-TDS-OFDM.

Fig. 9 the channel estimation performance of LABOMP with DPN, IBI free region and without IBI free region have been compared under real sparse time-varying UWA channel. In LABOMP without IBI free region full PN sequence has been used for channel estimation as in (15), in LABOMP with IBI free region the channel is estimated by using only the IBI free region in PN sequence as in (17), and in case of LABOMP with DPN the channel is estimated by using LABOMP CS algorithm based on the second PN sequence. The LABOMP with DPN outperforms than the LABOMP with IBI free region, at MSE equals to 10^{-2} and the SNR gain is almost 2 dB as seen in Fig. 9, due to the processing

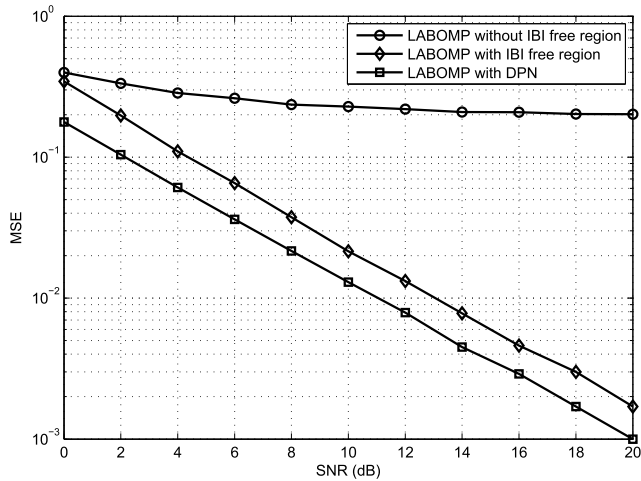


FIGURE 9. Channel estimation performance comparison of LABOMP without IBI free region, LABOMP with IBI free region and LABOMP with DPN for real sparse UWA channel K [1, 10].

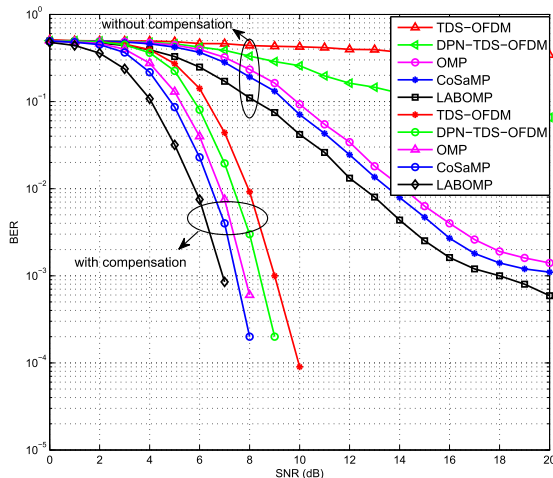


FIGURE 10. BER performance of different algorithms with and without CFO compensation for real sparse UWA channel K [1, 10].

of a large measurement matrix. But unfortunately, dual PN decreases the spectral and energy efficiency, which is very important for UWACs.

Fig. 10 shows the BER computation of LABOMP compared with TDS-OFDM, DPN-TDS-OFDM, OMP and CoSaMP in the real sparse UWA time-varying channel. The data is detected in frequency domain, where QPSK is used for demodulation, convolution and interleaving is used for decoding the data. LABOMP outperforms the conventional TDS-OFDM by about 2.15 dB, and the DPN-TDS by about 1.57 dB, also getting about 1.05 dB and 0.68 dB SNR gain compared with OMP and CoSaMP when target BER equals to 10^{-2} , respectively. Fig.10 portrays the BER performance in presence of Doppler compensation of the system. The BER performance after using compensation by the received PN is highly better in case of without Doppler compensation. When the SNR increased the BER is decreased quickly with the

TABLE 2. Comparison of spectral efficiency.

Guard Length	CP-OFDM	TDS-OFDM	DPN-TDS-OFDM	LABOMP
$N/4$	60.00%	80.00%	66.67%	80.00%
$N/8$	77.78%	88.89%	80.00%	88.89%
$N/16$	88.23%	94.12%	88.89%	94.12%

TABLE 3. Comparison of energy efficiency.

Guard Length	CP-OFDM	TDS-OFDM	DPN-TDS-OFDM	LABOMP
$N/4$	65.23%	66.67%	66.67%	94.12%
$N/8$	72.48%	80.00%	80.00%	96.97%
$N/16$	76.75%	88.89%	88.89%	98.46%

Doppler compensation. In general, LABOMP retains better performance with the compensation as well as without compensation than all of the conventional methods.

A. SPECTRAL EFFICIENCY

The OFDM systems spectral efficiency can be written as [15]:

$$\gamma_0 = \frac{N_{Data}}{N_{Data} + P_{Pilots}} \times \frac{N_{Frame}}{N_{Frame} + M} \times 100\% \quad (29)$$

where N_{Data} and P_{Pilots} represents the data size (data sub-carriers) and pilots sub-carriers, respectively. N_{Frame} is the frame length (data sub-carriers and pilots sub-carriers) and M is the length of guard interval. Table 2 compares the spectral efficiency of CP-OFDM, TDS-OFDM, DPN-TDS-OFDM, and LABOMP. Apart from reliable and fast synchronization, TDS-OFDM is more spectrally efficient than the CP-OFDM systems because of the removal of pilots. Here, the penalty for these merits is the essential to cancel the iterative interference due to the mutual interference between data block of OFDM and PN sequence. Twice the PN sequence in DPN-TDS-OFDM highly affected the spectral efficiency while utilizing CS into TDS-OFDM do not require alteration in the infrastructure of the system, so spectral efficiency can be inherited with better performance regarding MSE and BER.

B. ENERGY EFFICIENCY

The OFDM systems energy efficiency can be formulated as [15]:

$$Energy_{eff} = \frac{N_{Data}}{N_{Data} + b^2 P_{Pilots}} \times \frac{N_{Frame}}{N_{Frame} + a^2 M} \times 100\% \quad (30)$$

where, b represents the amplitude factor imposed on the pilots in frequency-domain and a represents the amplitude factor imposed on the guard interval in time domain. CP-OFDM is adopted to increase pilot amplitude that raises the performance of receiver channel estimation, e.g. $b = 4/3$ has been defined by the digital video broadcasting second generation terrestrial (DVB-T2) standard [15], [38]. Similarly, in TDS-OFDM system PN sequence amplitude is boosted to assure reliable channel estimation, DTMB standard specified the

value of $a = \sqrt{2}$ [15], [39]. On the contrary, the proposed LABOMP CS based TDS-OFDM with IBI free region can provide obviously improved channel estimation performance. LABOMP CS based method use the IBI free-region hence, it don't need a high power in the guard interval so the used training sequence amplitude is selected as $a = 0.5$. The energy efficiency of CP-OFDM, TDS-OFDM, DPN-TDS-OFDM, and LABOMP CS free-region IBI based are compared in Table 3. We have considered the typical example in CP-OFDM that the value of pilot occupation ratio is 11.29%, that is determined by the 4K mode of the DVB-T2 [38]. For DTMB standard amplitude factor is $a = \sqrt{2}$. In [19] amplitude factor is selected as $a = 1$ for the DPN-TDS-OFDM.

V. CONCLUSION

In this paper, a sparse channel estimation algorithm is proposed to mitigate IBI between data symbol and training sequence using LABOMP for underwater TDS-OFDM without modifying the TDS-OFDM frame structure. Thanks to the IBI free region in received PN training sequence, the LABOMP CS technique reconstruct the channel properly in order to obtain higher spectral and energy efficiency. Simulation results reveal that the proposed algorithm achieve significant performance enhancements. Due to the Doppler shift of the UWA channel, we have compensated the Doppler based on the received PN sequence in time domain before estimating the channel. The performance of the LABOMP is convincing and has given SNR gain of 4.29 dB and 5.89 dB in comparison of DPN-TDS-OFDM and conventional TDS-OFDM for considering MSE equal to 10^{-2} , LABOMOP also outperforms the CoSaMP and OMP by about 1.54 dB and 2.14 dB SNR gain, respectively. The simulation and numerical results depicts that the proposed LABOMP TDS-OFDM achieve better spectral efficiency, energy efficiency, and substantial MSE and BER improvement than the conventional OFDM systems.

REFERENCES

- [1] X. Ma, F. Yang, S. Liu, and J. Song, "Channel estimation for wideband underwater visible light communication: A compressive sensing perspective," *Opt. Express*, vol. 26, no. 1, pp. 311–321, Jan. 2018.
- [2] M. Mostafa, H. Esmaili, and E. M. Mohamed, "A comparative study on underwater communications for enabling C/U plane splitting based hybrid UWSNs," in *Proc. WCNC*, Apr. 2018, pp. 1–6.
- [3] I. Iglesias, A. Song, J. Garcia-Frias, M. Badié, and G. R. Arce, "Image transmission over the underwater acoustic channel via compressive sensing," in *Proc. 45th Annu. Conf. Inf. Sci. Syst.*, Baltimore, MD, USA, Mar. 2011, pp. 1–6.
- [4] Y. V. Zakharov and A. K. Morozov, "OFDM transmission without guard interval in fast-varying underwater acoustic channels," *IEEE J. Ocean. Eng.*, vol. 40, no. 1, pp. 144–158, Jan. 2015.
- [5] J. Li and Y. V. Zakharov, "Efficient use of space-time clustering for underwater acoustic communications," *IEEE J. Ocean. Eng.*, vol. 43, no. 1, pp. 173–183, Jan. 2018.
- [6] Z. Yang and Y. R. Zheng, "Iterative channel estimation and turbo equalization for multiple-input multiple-output underwater acoustic communications," *IEEE J. Ocean. Eng.*, vol. 41, no. 1, pp. 232–242, Jan. 2016.
- [7] C. R. Berger, Z. Wang, J. Huang, and S. Zhou, "Application of compressive sensing to sparse channel estimation," *IEEE Commun. Mag.*, vol. 48, no. 11, pp. 164–174, Nov. 2010.
- [8] S. Kaddouri, P.-P. J. Beaujean, and P.-J. Bouvet, "High-frequency acoustic estimation of time-varying underwater sparse channels using multiple sources and receivers operated simultaneously," *IEEE Access*, vol. 6, pp. 10569–10580, 2018.
- [9] L. Dai, Z. Wang, and Z. Yang, "Time-frequency training OFDM with high spectral efficiency and reliable performance in high speed environments," *IEEE J. Sel. Areas Commun.*, vol. 30, no. 4, pp. 695–707, May 2012.
- [10] H. Esmaili and D. Jiang, "Zero-pseudorandom noise training OFDM," *Electron. Lett.*, vol. 50, no. 9, pp. 650–652, 2014.
- [11] X. Ma, F. Yang, S. Liu, W. Ding, and J. Song, "Structured compressive sensing-based channel estimation for time frequency training OFDM systems over doubly selective channel," *IEEE Wireless Commun. Lett.*, vol. 6, no. 2, pp. 266–269, Apr. 2017.
- [12] B. Muquet, Z. Wang, G. Giannakis, M. de Courville, and P. Duhamel, "Cyclic prefixing or zero padding for wireless multicarrier transmissions?" *IEEE Trans. Commun.*, vol. 50, no. 12, pp. 2136–2148, Dec. 2002.
- [13] W. Jianming, Y. Chen, Z. Xiaoyang, and M. Hao, "Robust timing and frequency synchronization scheme for DTMB system," *IEEE Trans. Consum. Electron.*, vol. 53, no. 4, pp. 1348–1352, Nov. 2007.
- [14] W. Ding, F. Yang, W. Dai, and J. Song, "Time-frequency joint sparse channel estimation for MIMO-OFDM systems," *IEEE Commun. Lett.*, vol. 19, no. 1, pp. 58–61, Jan. 2015.
- [15] L. Dai, J. Wang, Z. Wang, P. Tsiaklakis, and M. Moonen, "Spectrum- and energy-efficient OFDM based on simultaneous multi-channel reconstruction," *IEEE Trans. Signal Process.*, vol. 61, no. 23, pp. 6047–6059, Dec. 2013.
- [16] J. Wang, Z.-X. Yang, C.-Y. Pan, S. Jian, and Y. Lin, "Iterative padding subtraction of the PN sequence for the TDS-OFDM over broadcast channels," *IEEE Trans. Consum. Electron.*, vol. 51, no. 4, pp. 1148–1152, Nov. 2005.
- [17] L. Ming, M. Crussiere, and J.-F. Hélaré, "A novel data-aided channel estimation with reduced complexity for TDS-OFDM systems," *IEEE Trans. Broadcast.*, vol. 58, no. 2, pp. 247–260, Jun. 2012.
- [18] M. Huemer, C. Hofbauer, and J. B. Huber, "Non-systematic complex number RS coded OFDM by unique word prefix," *IEEE Trans. Signal Process.*, vol. 60, no. 1, pp. 285–299, Jan. 2012.
- [19] J. Fu, J. Wang, J. Song, C.-Y. Pan, and Z.-X. Yang, "A simplified equalization method for dual PN-sequence padding TDS-OFDM systems," *IEEE Trans. Broadcast.*, vol. 54, no. 4, pp. 825–830, Dec. 2008.
- [20] L. Dai, Z. Wang, and Z. Yang, "Next-generation digital television terrestrial broadcasting systems: Key technologies and research trends," *IEEE Commun. Mag.*, vol. 50, no. 6, pp. 150–158, Jun. 2012.
- [21] S. Liu, F. Yang, W. Ding, and J. Song, "Double kill: Compressive-sensing-based narrow-band interference and impulsive noise mitigation for vehicular communications," *IEEE Trans. Veh. Technol.*, vol. 65, no. 7, pp. 5099–5109, Jul. 2016.
- [22] X. Ma, F. Yang, S. Liu, J. Song, and Z. Han, "Design and optimization on training sequence for mmWave communications: A new approach for sparse channel estimation in massive MIMO," *IEEE J. Sel. Areas Commun.*, vol. 35, no. 7, pp. 1486–1497, Jul. 2017.
- [23] L. Dai, Z. Wang, and Z. Yang, "Spectrally efficient time-frequency training OFDM for mobile large-scale MIMO systems," *IEEE J. Sel. Areas Commun.*, vol. 31, no. 2, pp. 251–263, Feb. 2013.
- [24] X. Ma, F. Yang, W. Ding, and J. Song, "Novel approach to design time-domain training sequence for accurate sparse channel estimation," *IEEE Trans. Broadcast.*, vol. 62, no. 3, pp. 512–520, Sep. 2016.
- [25] W. Ding, F. Yang, C. Pan, L. Dai, and J. Song, "Compressive sensing based channel estimation for OFDM systems under long delay channels," *IEEE Trans. Broadcast.*, vol. 60, no. 2, pp. 313–321, Jun. 2014.
- [26] C. R. Berger, S. Zhou, J. C. Preisig, and P. Willett, "Sparse channel estimation for multicarrier underwater acoustic communication: From subspace methods to compressed sensing," *IEEE Trans. Signal Process.*, vol. 58, no. 3, pp. 1708–1721, Mar. 2010.
- [27] Z. Liu and T. C. Yang, "On overhead reduction in time-reversed OFDM underwater acoustic communications," *IEEE J. Ocean. Eng.*, vol. 39, no. 4, pp. 788–800, Oct. 2013.
- [28] S. F. Mason, C. R. Berger, S. Zhou, and P. Willett, "Detection, synchronization, and Doppler scale estimation with multicarrier waveforms in underwater acoustic communication," *IEEE J. Sel. Areas Commun.*, vol. 26, no. 9, pp. 1638–1649, Dec. 2008.
- [29] B. Li, S. Zhou, M. Stojanovic, L. Freitag, and P. Willett, "Multicarrier communication over underwater acoustic channels with nonuniform Doppler shifts," *IEEE J. Ocean. Eng.*, vol. 33, no. 2, pp. 198–209, Apr. 2008.

[30] Z. Wang, L. Dai, and J. Wang, "Prior information aided compressive sensing for time domain synchronous OFDM," *Electron. Lett.*, vol. 48, no. 13, pp. 800–801, Jun. 2012.

[31] L. Dai, Z. Wang, and Z. Yang, "Compressive sensing based time domain synchronous OFDM transmission for vehicular communications," *IEEE J. Sel. Areas Commun.*, vol. 31, no. 9, pp. 460–469, Sep. 2013.

[32] C.-Y. Zeng, L.-H. Ma, M. H. Du, and J. Tian, "Regularized sequential selection and backtracking removal for CS atom matching," in *Proc. IEEE 14th Int. Workshop Multimedia Signal Process.*, Banff, AB, Canada, Sep. 2012, pp. 209–214.

[33] S. Chatterjee, D. Sundman, and M. Skoglund, "Look ahead orthogonal matching pursuit," in *Proc. IEEE Int. Conf. Acoust., Speech Signal Process. (ICASSP)*, Prague, Czech Republic, May 2011, pp. 4024–4027.

[34] D. L. Donoho, "Compressed sensing," *IEEE Trans. Inf. Theory*, vol. 52, no. 4, pp. 1289–1306, Apr. 2006.

[35] M. F. Duarte and Y. C. Eldar, "Structured compressed sensing: From theory to applications," *IEEE Trans. Signal Process.*, vol. 59, no. 9, pp. 460–4691, Sep. 2011.

[36] E. van den Berg and M. P. Friedlander, "Theoretical and empirical results for recovery from multiple measurements," *IEEE Trans. Inf. Theory*, vol. 56, no. 5, pp. 2516–2527, May 2010.

[37] Z. Yang, X. Wang, Z. Wang, J. Wang, and J. Wang, "Improved channel estimation for TDS-OFDM based on flexible frequency-binary padding," *IEEE Trans. Broadcast.*, vol. 56, no. 3, pp. 418–424, Sep. 2010.

[38] *Digital Video Broadcasting (DVB): Frame Structure Channel Coding and Modulation for a Second Generation Digital Terrestrial Television Broadcasting System (DVB-T2)*, ETSI, Standard EN 302 755, V1.3.1, Apr. 2012.

[39] *Error-Correction, Data Framing, Modulation and Emission Methods for Digital Terrestrial Television Broadcasting*, Standard Recommendation ITU-RBT.1306-5, Dec. 2011.



MINGZHANG ZHOU received the B.S. degree in communication engineering from the School of Information Science and Technology, Xiamen University, China, in 2017, where he is currently pursuing the master's degree. His research interests are channel coding and channel estimation for underwater acoustic communication, signal detection in OFDM, and signal processing.



HAIXIN SUN received the B.S. and M.S. degrees in electronic engineering from the Shandong University of Science and Technology, Shandong, China, in 1999 and 2003, respectively, and the Ph.D. degree in communication engineering from the Institute of Acoustic, Chinese Academy of Science, Shanghai, China, in 2006. He was a Visiting Scholar with the University of Connecticut, Hartford, CT, USA, in 2012. He is currently an Associate Professor with the School of Information Science and Technology, Xiamen University, China. His research interests include underwater acoustic communication and underwater acoustic signal processing.



nel estimation in OFDM, compressive sensing for wireless and underwater acoustic communication, signal detection, and signal processing.

NAVEED UR REHMAN JUNEJO received the B.S. degree in telecommunication engineering from the National University of Computer and Emerging Sciences (FAST-NUCES), Pakistan, in 2011, and the M.S. degree in information and communication engineering from Harbin Engineering University, China, in 2014. He is currently pursuing the Ph.D. degree with the School of Information Science and Technology, Xiamen University, China. His research interests are channel



JIE QI received the B.S. degree in automatic control and the M.S. degree in electronic engineering from Northwestern Polytechnical University, China, in 1995 and 1999, respectively, and the Ph.D. degree from the School of Aeronautics and Astronautics, Nanjing University of Aeronautics and Astronautics, Nanjing, China, in 2011. She is currently a Lecturer with the School of Information Science and Technology, Xiamen University. Her research is focused on optical sensing and optical communication.



Hamada Esmail, where he is currently an Assistant Professor with the Faculty of Engineering. His current research interests are 5G networks, cognitive radio networks, millimetre wave transmissions, and MIMO systems with an emphasis on multi-carrier for underwater communication systems. He is the General Co-Chair of the IEEE ITCE'18. He is a technical committee member in many international conferences and a reviewer in many international conferences, journals, and transactions.

HAMADA ESMAIEL (M'18) received the B.S. and M.S. degrees in electrical engineering from South Valley University, Aswan, Egypt, in 2005 and 2010, respectively, and the Ph.D. degree in wireless communication engineering from the School of Engineering, University of Tasmania, Hobart, TAS, Australia, in 2015. From 2007 to 2010, he was an Assistant Lecturer with South Valley University. In 2011, he was a Researcher Assistant with the Wireless Communication Laboratory, Wonkwang University, Iksan, South Korea. In 2011, he was an Assistant Researcher and a Lecturer with Aswan University, Aswan,



JUNFENG WANG received the Ph.D. degree in information and communication engineering from the School of Electronic Information Engineering, Tianjin University, China, in 2012. He joined the Tianjin University of Technology in 2012, where he is currently an Assistant Professor with the Department of Information and Communication Engineering, School of Electrical and Electronic Engineering. He is also a Visiting Researcher with the Missouri University of Science and Technology, USA. His current research interests include wireless communications and signal processing. He was a recipient of the 2008 Excellent Master Thesis Award and the 2012 Outstanding Graduate Research Achievement Award. He received the Best Paper Award at the 5th International Conference on Communications, Signal Processing, and Systems. He has served as a technical program committee member and a session chair for several IEEE/IET conferences, and as a reviewer of numerous IEEE/IET journals and conferences.

...